

Spatio-Temporal Characteristics of Ultrashort Pulses

Selcuk Akturk, Xun Gu and Rick Trebino

Introduction

So far in this book, our investigation of ultrafast optics has been limited to ideal one-dimensional ultrashort pulses in time (or equivalently in frequency). In this chapter, we will expand our treatment to a more general ultrashort beam-pulse, an entity that has both a transient temporal characteristic and a finite spatial extent, and in principle, these two dimensions may even be entangled. The full analysis of spatio-temporal characteristics of an ultrashort beam-pulse can theoretically be very complex; thus it is usually avoided by researchers whenever possible. However, as we will see later, many common lab apparatuses do routinely introduce spatio-temporal coupling into laser beams, and understanding the source, propagation and effect of the spatio-temporal coupling is essential to the design and operation of a successful laser experiment. Furthermore, the ability to control and manipulate the coupling between the temporal and spatial dimensions also offers a rarely explored avenue for new innovations in ultrafast optics research.

In this chapter, we will present a comprehensive view of linear spatio-temporal coupling in an ultrashort beam-pulse. We will first review the theory of ray optics using the $ABCD$ matrix approach [1], a convenient mathematical tool to model ray propagation. We will then introduce the Gaussian beam theory, a practical model to characterize the spatial distribution and angular divergence of a laser beam. Then, we will introduce an ultrashort-pulse extension of the $ABCD$ matrix formalism named the Kostenbauder-matrix (referred to as the K-matrix hereafter), which combines the temporal and spatial natures in the treatment of ultrafast ray-pulses. A further extension of the K-matrix to Gaussian beam-pulses is achieved in a new complex Q -matrix formalism. We will use this tool to construct a general theory for the description and propagation of the linear spatio-temporal couplings. Representations of beam-pulses in different domains are then discussed and the connections between these representations are revealed.

Common examples of spatio-temporal couplings

In this section, we will show some practical examples of spatio-temporal couplings in ultrafast laser beams, before attempting to establish a comprehensive mathematical description. We hope to convince the reader that spatio-temporal couplings are indeed commonplace occurrences in laser laboratories, and, as we will see later, that mathematical connections exist between various types of spatio-temporal couplings expressed in different domains.

We start with the null case, where no spatio-temporal couplings exist. This is indeed the default assumption behind most ultrafast optics discussions, in which main interest is given to the temporal behavior of the electromagnetic radiation, whereas the spatial dependence of the electric field is considered trivial and is thus accorded little or no attention.

The beam-pulse in the general context of ultrafast optics can be described by the electric field in space and time $E(x, y, z, t)$. As we know, the propagating electric field satisfies the wave equation

$$\left(\nabla^2 - \frac{1}{c^2} \frac{\partial^2}{\partial t^2} \right) E(x, y, z, t) = 0$$

Due to this constraint, there remain only three independent degrees of freedom for a propagating electromagnetic wave. In other words, if we know the electric field on a certain transverse plane $E(x, y, z=0, t)$, we may calculate the electric field $E(x, y, z, t)$ on any z planes simply by integrating the wave equation along z , using the Huygens' integral.

A beam-pulse is said to be *free of spatio-temporal couplings* on a z plane if the spatial dependence and the temporal dependence of the electric field can be separated, i.e.,

$$E(x, y, t) = E_{xy}(x, y) E_t(t)$$

where E_{xy} is the complex spatial profile function of the beam, and E_t is the complex temporal profile function of the pulse.

It is often useful and eliciting to consider alternative pictures of the electric field by Fourier-transforming the field expression from the space domain x, y and the time domain t into the corresponding reciprocal domains of spatial frequencies k_x, k_y and frequency ω . Obviously if the electric field is free of couplings in the space and time domains, it is also free of couplings in their reciprocal domains, or any hybrid domains.

The expression $E(x, y, \omega) = E_{xy}(x, y) E_\omega(\omega)$ shows that if a beam is free of spatio-temporal coupling, the spatial dependence of all frequency components in the pulse will be identical, in amplitude and in phase. This in fact holds true only for a collimated broadband pulse-beam for a relatively short distance, due to the fact that the diffraction of a laser beam is wavelength-dependent, and consequently, after a sufficiently long propagation distance, different frequency components will possess different beam sizes and destroy space-time separability. However, this particular divergence type of spatio-temporal coupling is usually fairly weak unless the spectral bandwidth in question is very broad. In our discussion of linear spatio-temporal couplings in this chapter, we will restrict ourselves to well-collimated beams that do not experience significant diffraction in the propagation distance to be involved.

A much stronger type of spatio-temporal coupling is the lateral displacement of different frequency components in a beam. This is usually called the **spatial chirp**, in analogy with the temporal chirp of an ultrashort pulse, which is the temporal displacement of different frequency components in the pulse.

Spatial chirp often results from propagating a beam with **angular dispersion** through a distance. Angular dispersion is a spatio-temporal distortion in the $k-\omega$ domain, i.e., different frequency (ω) components have different propagation directions (k). Angular dispersion can be introduced by passing a beam through a prism or a grating. This is very useful, because different frequency components are then separated along different directions (resulting in spatial chirp), and can be manipulated individually.

Propagating an angularly dispersed beam also introduces negative temporal chirp. This is the theoretical basis of a prism (or grating) pulse compressor [2], an extremely useful device in ultrafast optics. The device consists of two prisms (or gratings) aligned in an antiparallel way. The two prisms (or gratings) will cancel each other's angular dispersion, and the exiting beam will only have spatial chirp and the negative temporal chirp due to propagation with angular dispersion between the prisms (gratings). In order to remove the spatial chirp, the beam is often reflected back into the prism (grating) pair, or passed through an identical but opposite pair. The exiting beam will then have zero spatial chirp and zero angular dispersion, but twice the negative temporal chirp produced by a single prism (grating) pair.

It's easy to see why spatial chirp so frequently occurs as a result of a misaligned pulse compressor. The correct alignment of a prism (grating) compressor requires keeping the prism (grating) pair perfectly antiparallel, and reflecting the beam back into the prism (gratings) exactly on top of (or below) the incoming path. Any misalignment of the optics or the deviation of the incoming beam path will result in imperfect cancellation of spatial chirp or angular dispersion, and the exiting beam will be contaminated with spatio-temporal distortion.

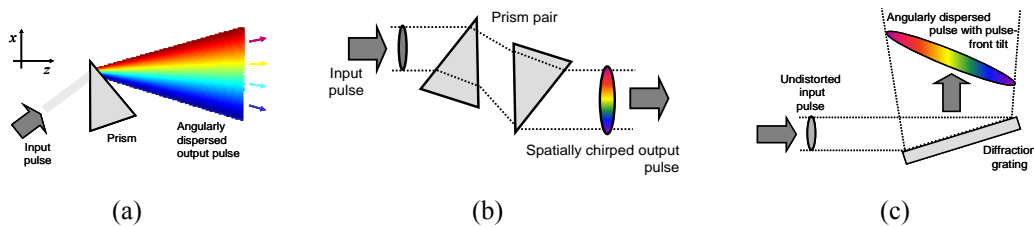


Fig. 1. Examples of (a) angular dispersion, (b) spatial chirp, and (c) pulse-front tilt.

Many other scenarios will also generate angular dispersion and spatial chirp. For example, nonlinear frequency conversion is commonly employed to produce new colors to be used in optics experiments. Efficient conversion usually requires phasematching, a strict condition between the wave vectors of all the optical waves involved, which, in anisotropic media including most nonlinear optical crystals, depends strongly on the propagation angles of the waves. Therefore, the generated signal beam will usually exhibit strong angular dispersion due to the wavelength and angular dependences of the phasematching condition, which will also turn into spatial chirp after propagation through some distance. This is a very common feature of broadband frequency conversion.

Another common type of spatio-temporal distortion can be defined in the $x-t$ domain, which is usually called the **pulse-front tilt**. In an ultrafast laser beam without spatio-temporal distortion, the pulse is temporally identical laterally across the beam (except for the relative spatial intensity variation), and the pulse arrives everywhere on the transverse plane at the same time. However, with the pulse-front tilt, the pulse arrives at different locations on the transverse plane at different times, forming a tilted pulse front. The beam coming off a grating will have pulse-front tilt as well as angular dispersion. Under some conditions, pulse-front tilt can be regarded as mathematically equivalent to angular dispersion, which is a well-known proof found in the literature [3, 4], but this is not always true in general [5], as we will find out later in this chapter.

Spatial chirp, angular chirp and pulse-front tilt are not the only types of spatio-temporal couplings. Obviously, after reviewing all possible commutations of variables, one would realize that there should exist one more type of coupling between k and t , whose physical meaning is more elusive. Furthermore, there are inherent connections among all these couplings which are not immediately clear; in other words, these couplings in different domains are not mutually independent.

In the rest of the chapter, we will introduce some necessary mathematical tools to describe rays, laser beams and pulses. A full spatio-temporal representation integrating elements of all these tools will be presented. Connections of spatio-temporal couplings in different domains will also be revealed. In all of these discussions, we will limit ourselves to only one spatial dimension x for the sake of simplicity. Inclusion of additional spatial dimensions is straightforward.

Ray Optics and $ABCD$ Matrices

Let's first focus on rays, and introduce a basic ray-tracing tool called the ray matrix, or the $ABCD$ matrix. We will see in later sections that these basic $ABCD$ matrices can be further extended and be used to even describe Gaussian laser beams and laser pulses, allowing for a simple yet powerful way of treating optical systems.

The ray is a mathematical straight line symbolizing an idealized narrow beam of light. We use this concept to model the propagation of light, in such cases where we can disregard its wave (diffraction) properties. As we know, the definition of a line requires two independent parameters: the slope and the

intercept. This can be written in a vector form $\begin{pmatrix} x \\ \theta \end{pmatrix}$, where x is the lateral position of the ray, and

$\theta = \frac{dx}{dz}$ is the slope (ray angle).

The propagation of a ray through an optical system is simply modeled as a linear transformation of

the ray vector elements $\begin{pmatrix} x_{\text{out}} \\ \theta_{\text{out}} \end{pmatrix} = \begin{pmatrix} A & B \\ C & D \end{pmatrix} \begin{pmatrix} x_{\text{in}} \\ \theta_{\text{in}} \end{pmatrix}$, where the matrix $T = \begin{pmatrix} A & B \\ C & D \end{pmatrix}$ is called the **$ABCD$**

matrix (ray matrix) of the optical system.

It is easily seen that a composite optical system comprising n subsystems will have an $ABCD$ matrix of $T = T_n T_{n-1} \cdots T_1$, where T_1 is the $ABCD$ matrix of the first subsystem at the input, and T_n is that of the last subsystem at the output. This cascaded system matrix T fully captures the behavior of the system in terms of *spatial* manipulation of rays.

Gaussian Beams

Rays are an idealized and often oversimplified model of light propagation. In reality, a laser emits a beam of finite width, and the beam will naturally diverge with propagation due to diffraction, which is a physical optics phenomenon unable to be described by rays. Understanding the physics of the beam size, propagation and divergence is very important in the practical manipulation of real laser beams.

We will not go into the mathematical details of solving the wave equation in space. The interested reader is referred to standard textbooks such as *Lasers* by A. Siegman for more mathematically involved discussions. Suffice it to say here that there exist solutions of the wave equation that are mathematically appealing and are of great practical values. Perhaps the most useful of such solutions, under the so-called paraxial approximation, are the Hermite-Gaussian modes in the Cartesian coordinate system, and the Laguerre-Gaussian modes in the cylindrical coordinate system. These modes constitute a complete orthogonal basis for the expansion of any beam near the optical axis, under the paraxial approximation. Note in this section, only a monochromatic laser beam is covered.

The lowest-order solutions of both the Hermite-Gaussian modes and the Laguerre-Gaussian modes are the same, having a particularly simple mathematical form (assuming the optical axis is the z -axis),

$$E(x, y, z) = \frac{1}{q(z)} \exp \left[-ik \frac{x^2 + y^2}{2q(z)} \right]$$

where $\frac{1}{q(z)} = \frac{1}{q(0) + z} \equiv \frac{1}{R(z)} - i \frac{\lambda}{\pi w^2(z)}$ is a complex parameter.

It is easy to see that the transverse field distribution on any z -plane is a Gaussian function, with $w(z)$ being the $1/e^2$ -intensity radius of the beam. $R(z)$, on the other hand, is the radius of curvature of the wave front at z .

Beams of this profile are referred to as Gaussian beams in the rest of this chapter, and will be the assumption in our further studies. This simplification is very useful. Most practical (and useful) laser beams are indeed, to a very large extent, Gaussian beams, and can be very accurately described by the rules of Gaussian beams. However, as an exception, one should exert caution when dealing with tightly-focused beams, when the paraxial approximation does begin to break down.

For a Gaussian beam, there always exists a particular z_0 , which renders

$$\frac{1}{q(z_0)} = \frac{1}{R(z_0)} - i \frac{\lambda}{\pi w_0^2} = -i \frac{\lambda}{\pi w_0^2} \text{ purely imaginative.}$$

This location is called the beam waist,

and $w_0 = w(z_0)$ is called the spot size of the waist. The beam waist is the z -plane where the beam has the smallest diameter. The beam diameter gradually grows as we move away from the waist plane.

It is easy to see from the formula above that the expansion of the beam size is not uniform with the departure from the waist. In the immediate region close to the beam waist, the beam size does not change much; far away from the waist, however, the beam size grows nearly proportionally to the departure from the beam waist. Figure 2 shows a typical picture of beam divergence.

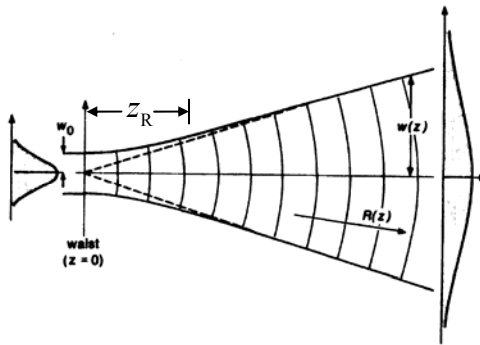


Fig. 2. Gaussian beam divergence.

It is customary to define the Raleigh range $z_R = \frac{\pi w_0^2}{\lambda}$ to qualitatively demark the boundaries between the two regions where beam divergence behaves differently. At $z = z_0 \pm z_R$, the beam diameter is $\sqrt{2}$ times the diameter at the beam waist.

In the far field, the beam diverges linearly with propagation, with a half divergence angle given by $\theta = \frac{\lambda}{\pi w_0}$.

Gaussian beams undergo transformations as they go through optical systems. It is possible to derive, by using the Huygens' integral, that after a paraxial system described by an arbitrary $ABCD$ matrix (which can even be complex-valued), the output beam remains Gaussian, and the complex q parameter of the output beam is given by,

$$q_{\text{out}} = \frac{Aq_{\text{in}} + B}{Cq_{\text{in}} + D}$$

This rule of Gaussian beam transformation is extremely useful, as it permits the calculation of Gaussian beam propagation through a series of optical systems, using only the cascaded $ABCD$ matrix elements. It will be the basis of our spatio-temporal analysis in the upcoming sections.

Kostenbauder matrices

The discussions above have all assumed a monochromatic beam; therefore only the spatial aspect of the laser radiation is covered. With a range of frequency components that an ultrashort laser pulse necessarily contains, it is imperative to add a few more parameters in the model of optical systems, in order to include not only the temporal dispersion of the pulse due to the system, but also the spatio-temporal coupling that may exist between the two independent arguments of space and time.

A theory that integrates the ray analysis and the temporal dispersion calculations in one framework was developed by A. G. Kostenbauder [6]. In this theory, a 4-element vector $\begin{bmatrix} x \\ \theta \\ t \\ \nu \end{bmatrix}$ is used to represent a

ray-pulse, an entity that has both the spatial parameters of a ray and the temporal and spectral parameters of a Gaussian-shaped pulse, where x is the lateral position, θ is the propagation angle, t is the group delay and ν is the center frequency of the pulse.

The effect of an optical system on the propagation of a ray-pulse is represented by a 4x4 matrix called the Kostenbauder matrix or the K-matrix. The transformation of the ray-pulse parameters through the optical system is a simple matrix multiplication.

$$\begin{bmatrix} x_{\text{out}} \\ \theta_{\text{out}} \\ t_{\text{out}} \\ \nu_{\text{out}} \end{bmatrix} = \begin{bmatrix} A & B & 0 & E \\ C & D & 0 & F \\ G & H & 1 & I \\ 0 & 0 & 0 & 1 \end{bmatrix} \begin{bmatrix} x_{\text{in}} \\ \theta_{\text{in}} \\ t_{\text{in}} \\ \nu_{\text{in}} \end{bmatrix}$$

The K-matrix of a cascaded paraxial system is again the matrix product of the K-matrices of subsystems, applying the same rule as for ABCD matrices.

It is easy to identify the physical meanings of the five additional matrix elements, in a *ray-pulse picture*:

$$E = \frac{\partial x_{\text{out}}}{\partial \nu_{\text{in}}} \text{ signifies spatial chirp,}$$

$$F = \frac{\partial \theta_{\text{out}}}{\partial \nu_{\text{in}}} \text{ signifies angular chirp,}$$

$$G = \frac{\partial t_{\text{out}}}{\partial x_{\text{in}}} \text{ signifies pulse-front tilt,}$$

$$H = \frac{\partial t_{\text{out}}}{\partial \theta_{\text{in}}} \text{ is a time-vs.-angle coupling term,}$$

$$I = \frac{\partial t_{\text{out}}}{\partial \nu_{\text{in}}} \text{ signifies group-delay dispersion.}$$

Using the K-matrices, the propagation of a Gaussian laser pulse through a paraxial linear-dispersion system can be easily calculated. However, in this approach, light is treated as rays, so there is no spatial overlap between different frequency components, which can be an important aspect of spatio-temporal couplings in real-world laser beams. A more complete spatio-temporal treatment concerning Gaussian *beams* will be given in the next section.

Propagating a beam-pulse: the complex Q-matrix

As we have seen in the previous section, the 4x4 K-Matrices can be very useful in modeling propagation of ultrashort pulses through linear optical systems, consisting of number of elements, including dispersive ones. This formalism is suitable for transforming a “ray-pulse”. In other words, the finite extent of a laser beam is not taken into account. In this section, we will consider pulses with finite beam sizes and extend the matrix approach to the propagation of a “beam-pulse”. In order to be able to derive analytical results, we will assume Gaussian spatial and temporal beam-pulse profiles.

A Gaussian beam-pulse can be written in the form:

$$E(x, t) = \exp \left\{ -i \frac{\pi}{\lambda_0} \begin{pmatrix} x \\ -t \end{pmatrix}^T Q^{-1} \begin{pmatrix} x \\ t \end{pmatrix} \right\} = \exp \left[-i \frac{\pi}{\lambda_0} \left((Q^{-1})_{11} x^2 + (Q^{-1})_{12} xt - (Q^{-1})_{21} xt - (Q^{-1})_{22} t^2 \right) \right] \quad (1)$$

where $(Q^{-1})_{12} = -(Q^{-1})_{21}$, so we will combine these two quantities in all future results.

Equation (1) can be written in a more compact manner by absorbing the constant and inverses in the tilde symbol, and substituting the indices with coordinates:

$$E(x, t) \propto \exp \left\{ \tilde{Q}_{xx} x^2 + 2\tilde{Q}_{xt} xt - \tilde{Q}_{tt} t^2 \right\} \quad (2)$$

The diagonal elements of \tilde{Q} can be easily recognized from Gaussian beams and pulses:

$$\tilde{Q}_{xx} = -i \frac{\pi}{\lambda R(z)} - \frac{1}{w^2(z)} \quad (3)$$

$$\tilde{Q}_{tt} = -i\beta + \frac{1}{\tau^2} \quad (4)$$

where λ is the pulse center wavelength, R is the beam radius of curvature, w is the spot size, β is temporal chirp and τ is temporal pulse width. The off-diagonal element describes the coupling between space and time. Therefore the real part of \tilde{Q}_{xt} term gives the pulse-front tilt.

Analogously to the complex q parameter used in beam propagation with ABCD matrices, we can construct a complex Q matrix. At the input of an optical system, the Q matrix is:

$$Q_{in} = \begin{bmatrix} Q_{11} & Q_{12} \\ -Q_{12} & Q_{22} \end{bmatrix} = i \frac{\lambda}{\pi} \begin{bmatrix} \tilde{Q}_{xx} & \tilde{Q}_{xt} \\ -\tilde{Q}_{xt} & \tilde{Q}_{tt} \end{bmatrix}^{-1} \quad (5)$$

Now, we can propagate the complex Q matrix, (hence the pulse electric field) using the K-matrix, by using the propagation expression:

$$Q_{out} = \left\{ \begin{bmatrix} A & 0 \\ G & 1 \end{bmatrix} Q_{in} + \begin{bmatrix} B & E/\lambda_0 \\ H & I/\lambda_0 \end{bmatrix} \right\} \cdot \left\{ \begin{bmatrix} C & 0 \\ 0 & 0 \end{bmatrix} Q_{in} + \begin{bmatrix} D & F/\lambda_0 \\ 0 & 1 \end{bmatrix} \right\}^{-1} \quad (6)$$

Even though Equation (6) looks a bit complicated, it is still easier to use than the equivalent Huygens integral formalism. Besides, this matrix approach has the additional advantage that, a beam-pulse can be propagated through several elements by first finding the overall K-matrix for the systems and then using the propagation expression.

The general theory of the spatio-temporal couplings

So far we talked about various spatio-temporal couplings resulting from the use of dispersive optical elements. Even though these spatio-temporal couplings correspond to different phenomena, they are not at all independent from each other. As we will see in this section, many of these couplings are closely related. In this section, we will be answering two basic questions: 1) What are the possible spatio-temporal couplings and 2) What are the relations between different couplings. Answering these questions will give us a general and complete picture of the first order spatio-temporal couplings.

To answer these two questions, we investigate all possible coupling effects in the various possible domains, and we derive analytical expressions that, not only properly describe them, but also yield explicit relations between different effects. We consider beams that are Gaussian in the transverse spatial (x) domain and hence also in its Fourier conjugate domain (k). We also consider pulses that are Gaussian in time (t) and hence also in frequency (ω).

Our approach will be as follows: we will start with the expression in Eq.(2). Equation (2) inherently contains the full space-time pulse information (up to second order). We will then calculate the electric field in other domains, namely, the (x,ω) , (k,ω) and (k,t) domains by performing (inverse) Fourier transforms. In each domain we will identify coefficients like the Q s in the (x,t) domain. The cross terms in each domain will be the spatio-temporal couplings in that particular domain. This will determine essentially all of the possible first-order couplings as well as the relations between them.

We concentrate on only one transverse spatial coordinate, the transverse 'x', as generalization to both transverse coordinates (x and y) is trivial. Also, one could easily generalize our formalism to an arbitrary spatial and/or temporal profile by using computational methods.

Expressing the pulse in different domains

The electric field as expressed in Eq. (2):

$$E(x,t) \propto \exp \left\{ \tilde{Q}_{xx} x^2 + 2\tilde{Q}_{xt} xt - \tilde{Q}_{tt} t^2 \right\}$$

contains the spatio-temporal beam-pulse information. The real and imaginary parts of each of the Q elements correspond to distinct physical parameters. As can be inferred from Eq.s (3) and (4), the cross terms correspond to:

$$\begin{aligned}
\text{Re}\{\tilde{Q}_{xx}\} &\leftrightarrow \text{beam spot size (BSS)} \\
\text{Im}\{\tilde{Q}_{xx}\} &\leftrightarrow \text{wave-front curvature (WFC)} \\
\text{Re}\{\tilde{Q}_{tt}\} &\leftrightarrow \text{temporal pulse width (TPW)} \\
\text{Im}\{\tilde{Q}_{tt}\} &\leftrightarrow \text{temporal chirp (TCH)}
\end{aligned} \tag{7}$$

The spatio-temporal coupling information is within the cross term. Because the pulse intensity profile is given by the squared magnitude of the E-field, the real part of Q_{xt} yields a position-time coupling in the intensity profile vs. x and t . This phenomenon is the aforementioned pulse-front tilt (PFT). The imaginary part of Q_{xt} , on the other hand, yields a time-and-position-dependent *phase*. Physically, this phase distortion causes the wave-front of the pulse to *rotate in time*, so it can be named as “wave-front rotation” (WFR). We then write:

$$\begin{aligned}
\text{Re}\{\tilde{Q}_{xt}\} &\leftrightarrow \text{pulse-front tilt (PFT)} \\
\text{Im}\{\tilde{Q}_{xt}\} &\leftrightarrow \text{wave-front rotation (WFR)}
\end{aligned} \tag{8}$$

The field can now be Fourier transformed to the (x,ω) domain to find the couplings in that domain:

$$E(x, \omega) = \frac{1}{2\pi} \int E(x, t) e^{-i\omega t} dt \tag{9}$$

Carrying out the integral, we get an equation in the same form of Eq. (2), but with a new set of coefficients:

$$E(x, \omega) \propto \exp\{R_{xx}x^2 + 2R_{x\omega}x\omega - R_{\omega\omega}\omega^2\} \tag{10}$$

Following the same arguments, we can identify the physical meaning of these coefficients:

$$\begin{aligned}
\text{Re}\{R_{xx}\} &\leftrightarrow \text{beam spot size (BSS)} \\
\text{Im}\{R_{xx}\} &\leftrightarrow \text{wave-front curvature (WFC)} \\
\text{Re}\{R_{\omega\omega}\} &\leftrightarrow \text{bandwidth (BDW)} \\
\text{Im}\{R_{\omega\omega}\} &\leftrightarrow \text{frequency chirp (FCH)} \\
\text{Re}\{R_{x\omega}\} &\leftrightarrow \text{spatial chirp (SPC)} \\
\text{Im}\{R_{x\omega}\} &\leftrightarrow \text{wave-front-tilt dispersion (WFD)}
\end{aligned} \tag{11}$$

The real part of the coupling term, $R_{x\omega}$, yields position dependent spectrum, the well-known spatial chirp. The imaginary part of $R_{x\omega}$ causes the wave-front to be tilted by an amount that depends on the frequency: “wave-front-tilt dispersion” (WFD).

Next, we inverse-Fourier-transform Eq. (10) to the (k,ω) domain:

$$E(k, \omega) \propto \exp\{S_{kk}k^2 + 2S_{k\omega}k\omega - S_{\omega\omega}\omega^2\} \tag{12}$$

And the S coefficients are:

$$\begin{aligned}
\text{Re}\{S_{kk}\} &\leftrightarrow \text{angular divergence (ADV)} \\
\text{Im}\{S_{kk}\} &\leftrightarrow \text{angular phase-front curvature (APC)} \\
\text{Re}\{S_{\omega\omega}\} &\leftrightarrow \text{bandwidth (BDW)} \\
\text{Im}\{S_{\omega\omega}\} &\leftrightarrow \text{frequency chirp (FCH)} \\
\text{Re}\{S_{k\omega}\} &\leftrightarrow \text{angular dispersion (AGD)} \\
\text{Im}\{S_{k\omega}\} &\leftrightarrow \text{angular spectral chirp (ASC)}
\end{aligned} \tag{13}$$

The real off-diagonal parameter, $\text{Re}\{S_{k\omega}\}$, causes frequency dependent propagation angle: the angular dispersion. The imaginary part, $\text{Im}\{S_{k\omega}\}$, involves a variation in the frequency with angle, hence called “angular spectral chirp” (ASC).

Finally, we inverse Fourier-transform Eq. (12) to the (k,t) domain:

$$E(k, t) \propto \exp\{P_{kk}k^2 + 2P_{kt}kt + P_{tt}t^2\} \quad (14)$$

And the P coefficients are:

$$\begin{aligned} \text{Re}\{P_{kk}\} &\leftrightarrow \text{angular divergence (ADV)} \\ \text{Im}\{P_{kk}\} &\leftrightarrow \text{angular phase-front curvature (APC)} \\ \text{Re}\{P_{tt}\} &\leftrightarrow \text{temporal pulse width (TPW)} \\ \text{Im}\{P_{tt}\} &\leftrightarrow \text{temporal chirp (TCH)} \\ \text{Re}\{P_{kt}\} &\leftrightarrow \text{time vs. angle (TVA)} \\ \text{Im}\{P_{kt}\} &\leftrightarrow \text{angular temporal chirp (ATC)} \end{aligned} \quad (15)$$

The real off-diagonal parameter here, $\text{Re}\{P_{kt}\}$, is the pulse “time vs. angle,” (TVA). The imaginary coupling term is “angular temporal chirp” (ATC).

Defining widths in presence of spatio-temporal couplings

Defining the widths (i.e. the beam spot size, pulse width, bandwidth, and divergence angle) becomes tricky when the spatio-temporal couplings are present. In the presence of pulse-front tilt, for example, the beam central position will depend on time and the spot size at a given time will be less than the spot size integrated over all times. There are thus two types of width, one at a given time and another integrated over all time, as well as position. Since the intensity profile is usually measured with slow detectors, the intensity profile $I(x,t)$ is usually integrated over time, as well. This will yield what could be called a “global” spot size (indicated by the subscript “G”), as opposed to the spot size at a given time, which is the “local” spot size, (and henceforth indicated by the subscript “L”). Using the root-mean-square definition, we can find the beam widths as:

$$\Delta x_L(t) = \left[\frac{\int x^2 I(x,t) dx - \left(\int x I(x,t) dx \right)^2}{\int I(x,t) dx} \right]^{1/2} = \left[-\frac{1}{4\tilde{Q}_{xx}^R} \right]^{1/2} \quad (16)$$

$$\Delta x_G = \left[\frac{\iint x^2 I(x,t) dx dt}{\iint I(x,t) dx dt} \right]^{1/2} = \frac{1}{2} \left[-\frac{\tilde{Q}_{tt}^R}{\tilde{Q}_{xx}^R \tilde{Q}_{tt}^R + \tilde{Q}_{xt}^R} \right]^{1/2} \quad (17)$$

And the pulse widths as:

$$\begin{aligned} \Delta t_L &= \left[\frac{1}{4\tilde{Q}_{tt}^R} \right]^{1/2} \\ \Delta t_G &= \frac{1}{2} \left[\frac{\tilde{Q}_{xx}^R}{\tilde{Q}_{xx}^R \tilde{Q}_{tt}^R + \tilde{Q}_{xt}^R} \right]^{1/2} \end{aligned} \quad (18)$$

Widths in other domains can be found simply by substituting \tilde{Q} s with the corresponding coefficients in the particular domain.

Defining and normalizing the spatio-temporal couplings

We have identified the real parts of the cross terms in each domain as equivalent to the known spatio-temporal couplings. However, for experimental convenience and better intuition, normalization is helpful. As an example, we will work in (x, ω) domain and express the spatial chirp in terms of the various coefficients of the R matrix. Generalization to other domains is trivial.

Spatial chirp can be visualized in two alternate ways: frequency dependent center position or position dependent center frequency. The former was defined as the “spatial dispersion (SPD),” $\partial x_0 / \partial \omega$, where x_0 is the mean beam position for a given frequency, ω . The latter is the “frequency gradient (FRG),” $\partial \omega_0 / \partial x$, where ω_0 is the mean frequency for a given position, x . To be able to express $R_{x\omega}$ in terms of the spatial dispersion or the frequency gradient, we must normalize it with respect to the beam width or frequency bandwidth. This requires rearranging the exponential in Eq. (10):

$$\begin{aligned} E(x, \omega) &\propto \exp \left[R_{xx}^R \left(x + \frac{R_{x\omega}^R}{R_{xx}^R} \omega \right)^2 - \left(\frac{R_{x\omega}^R{}^2}{R_{xx}^R} + R_{\omega\omega}^R \right) \omega^2 \right] \\ &= \exp \left[- \left(\frac{x - \frac{\partial x_0}{\partial \omega} \omega}{4\Delta x_L} \right)^2 - \frac{\omega^2}{4\Delta \omega_G^2} \right] \end{aligned} \quad (19)$$

where we have used a shortcut notation, superscript “ R ”, for the real part of the parameter. Hence, we can readily see that spatial dispersion is the cross term normalized by the beam width:

$$\frac{\partial x_0}{\partial \omega} = - \frac{R_{x\omega}^R}{R_{xx}^R} \quad (20)$$

Similarly, we can arrange the exponential in a slightly different form:

$$\begin{aligned} E(x, \omega) &= \exp \left[- \frac{x^2}{4\Delta x_G^2} - \left(\frac{\omega - \frac{\partial \omega_0}{\partial x} x}{4\Delta \omega_L} \right)^2 \right] \\ &= \exp \left[\left(\frac{R_{x\omega}^R{}^2}{R_{\omega\omega}^R} + R_{xx}^R \right) x^2 - R_{\omega\omega}^R \left(\omega - \frac{R_{x\omega}^R}{R_{\omega\omega}^R} x \right)^2 \right] \end{aligned} \quad (21)$$

And notice that the frequency gradient is the cross term normalized by the bandwidth:

$$\frac{\partial \omega_0}{\partial x} = \frac{R_{x\omega}^R}{R_{\omega\omega}^R} \quad (22)$$

We can also derive a relation between the two definitions of spatial chirp:

$$\frac{\partial \omega_0}{\partial x} = \frac{\frac{\partial x_0}{\partial \omega}}{\left(\frac{\partial x_0}{\partial \omega} \right)^2 + \frac{\Delta x_L^2}{\Delta \omega_G^2}} \quad (23)$$

There is yet another possible way of normalizing the spatial chirp. It can be expressed as a dimensionless quantity, considered as a type of “correlation coefficient,” by normalizing with respect to both beam width and bandwidth:

$$\rho_{x\omega} \equiv \frac{\iint x\omega I(x, \omega) dx d\omega}{\iint I(x, \omega) dx d\omega} \frac{1}{\Delta x_G \Delta \omega_G} = \frac{R_{x\omega}^R}{\sqrt{-R_{xx}^R R_{\omega\omega}^R}} \quad (24)$$

Defining the coupling in terms of these correlation coefficients has an advantage that the coefficient ρ always lies between 1 and -1. Therefore, this quantity can easily show whether the coupling is “large” or “small.” It is also possible to relate the global and local widths by the correlation coefficient:

$$\begin{aligned}\Delta x_L(\omega) &= \Delta x_G \sqrt{1 - \rho_{x\omega}^2} \\ \Delta \omega_L(x) &= \Delta \omega_G \sqrt{1 - \rho_{x\omega}^2}\end{aligned}\quad (25)$$

Note that obtaining more intuitive, normalized quantities like SPD, FRG and $\rho_{x\omega}$ only involves division of the cross term by the beam width or the bandwidth or both.

This same approach can be directly applied to the other three domains. Analogously to SPD and FRG, for example, PFT can be viewed as the “arrival time (of maximum or mean intensity) vs. position” or “position (of maximum or mean intensity) vs. time.”

Relations between the spatio-temporal couplings

So far we saw that, to first order, there are four distinct real (amplitude) spatio-temporal couplings: PFT, SPC, AGD and TVA, and there are four imaginary (phase) spatio-temporal couplings: WFR, WFD, ASC and ATC. Obviously, they are not all independent. In fact, if one has all six (three real and three imaginary) coefficients in any single domain, then the field in all other domains can be calculated by taking Fourier transforms. Thus, there are only two independent spatio-temporal couplings! The other six can be computed from these two (and the relevant diagonal components, such as the pulse width, temporal chirp, spot size, and wave-front radius of curvature).

The relations between the coefficients in different domains result directly from the Fourier transforms that we used in the previous sections. These relations are summarized in table 1 below. Each row of the table shows the cross terms in one domain and its equivalent representation in the others.

Table 1. Summary of the relations of spatio-temporal couplings in all four domains.

(x,t)	(x, ω)	(k, ω)	(k,t)
\tilde{Q}_{xt}	$\frac{i R_{x\omega}}{2 R_{\omega\omega}}$	$\frac{1}{4} \frac{S_{k\omega}}{S_{kk} S_{\omega\omega} + S_{k\omega}^2}$	$-\frac{i P_{kt}}{2 P_{kk}}$
$-\frac{i \tilde{Q}_{xt}}{2 \tilde{Q}_{tt}}$	$R_{x\omega}$	$-\frac{i S_{k\omega}}{2 S_{kk}}$	$\frac{1}{4} \frac{P_{kt}}{P_{kk} P_{tt} + P_{kt}^2}$
$\frac{1}{4} \frac{\tilde{Q}_{xt}}{\tilde{Q}_{xx} \tilde{Q}_{tt} + \tilde{Q}_{xt}^2}$	$\frac{i R_{x\omega}}{2 R_{xx}}$	$S_{k\omega}$	$-\frac{i P_{kt}}{2 P_{tt}}$
$\frac{i \tilde{Q}_{xt}}{2 \tilde{Q}_{xx}}$	$\frac{1}{4} \frac{R_{x\omega}}{R_{xx} R_{\omega\omega} + R_{x\omega}^2}$	$\frac{i S_{k\omega}}{2 S_{\omega\omega}}$	P_{kt}

We can use this complete table of relations to derive intuitive expressions. For example, if the beam is well collimated, the R_{xx} term can be assumed to be real (the imaginary part approaches zero when radius of curvature is very large). Then, using table 1, the real part of $S_{k\omega}$ (AGD) will be proportional to the imaginary part of $R_{x\omega}$ (WFD). Therefore, in the well-collimated-beam approximation, we can conclude that $R_{x\omega}^I$ is proportional to AGD. If we express PFT in its form normalized only by the pulse width, we can write:

$$\text{PFT} = \text{AGD} + 2 \text{FCH} \times \text{FRG} \quad (26)$$

We can translate Eq. (26) to words: “pulse-front tilt is generated by angular dispersion and simultaneous spatial and temporal chirp”. Similar expressions can be easily derived for other couplings.

Constructing the electric field in different domains

To be able to explicitly write the pulse electric field in one of the domains, one needs only six independent parameters (real and imaginary parts of the coefficients). Namely, in (x,t) domain, one needs BSS, WFC, TPW, TCH, PFT and WFR. The spatial and temporal parameters, as well as PFT can be measured with well established pulse characterization methods. However, directly measuring WFR is not easy. In general, it is experimentally easier to measure intensity couplings, than phase couplings. Therefore it would be very useful if we could express WFR (or other phase couplings) in terms of the intensity couplings. Using the relations in table 1, we can derive:

$$\text{WFR} = \frac{\text{FRG}}{2} + \text{TCH} \times \text{PFT} \quad (27)$$

In this expression, the PFT is normalized only by the pulse width. Therefore, in addition to the pulse spatial and temporal parameters and PFT, if one knows the FRG as well, then the complete Gaussian beam-pulse field is known. It is also possible to derive analogous expression for the phase couplings in the other domains. They can be expressed in terms of the intensity couplings in the adjacent domains.

In the figures below, we illustrate the ideas of this section. Starting only with the six parameters mentioned above, we constructed the pulse electric field in all four domains. Figure 1 shows the intensity profiles of such a pulse in the various domains. The intensity traces are tilted in each of the four domains, indicating the presence of all four spatio-temporal couplings. Table 2 show the spatio-temporal couplings in each domain expressed in terms of dimensionless correlation coefficients. Note that the correlation coefficients intuitively describe both the magnitude and sign of the couplings.

The input parameters for the pulse shown in figure 1 are as follows: Center wavelength = 800 nm, $\Delta x_G = 2.56$ mm, $\Delta t_G = 82.1$ fs, $\text{TCH} = 6.2 \times 10^{-4}$ fs⁻². And coupling values are $\text{PFT} = 7$ fs/mm, $\text{SPD} = 3.4$ mm.fs/rad. These values of PFT and SPD correspond to the following experimental situation: an anti-parallel prism pair, each prism made of fused silica with apex angles of 69 degree. The prisms are separated by 310 mm. The first prism is used at Brewster’s angle and the second one is tilted from Brewster’s angle by 1.5 degrees.

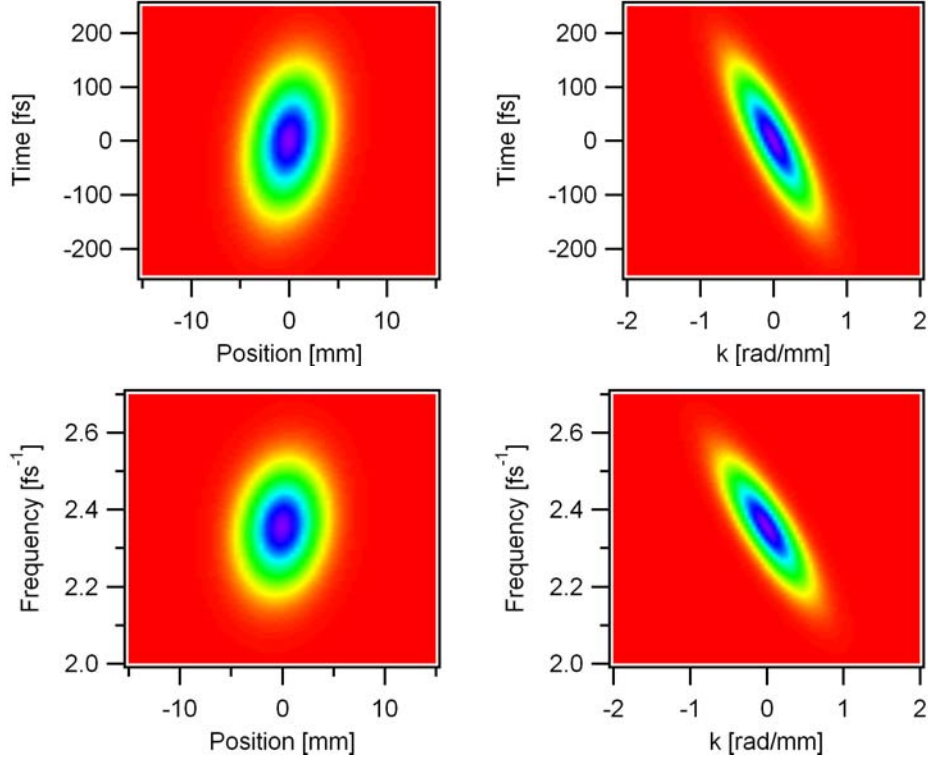


Fig.1. Intensity profile of a pulse expressed in the four different domains. This pulse simultaneously has all four spatio-temporal amplitude couplings: PFT, SPC, AGD and TVA, as can be seen from the tilted images.

Table 2 The correlation coefficients of the pulse field shown in Figure 3.

Coupling	ρ_{xt}	ρ_{kt}	$\rho_{x\omega}$	$\rho_{k\omega}$
value	0.22	-0.81	0.14	-0.82

Wigner Distributions

In the previous sections, we saw the 4x4 K-matrix formalism and a general approach of defining spatio-temporal couplings. In most of the analysis so far, we assumed Gaussian beam and pulse profiles. However, if the beam-pulse shape is non-Gaussian, it is more difficult to propagate a beam-pulse through an optical system and to analyze the spatio-temporal behavior. One way of doing this is to evaluate the Fresnel-Kirchoff integral. This usually requires somewhat complicated computer computation.

In this section, we will talk about an alternative way of representing ultrashort pulses with arbitrary profiles, called “Wigner Distributions”. These functions have very interesting mathematical properties and they yield intuitive pictures of pulses possessing spatio-temporal couplings. Furthermore, we will see that, propagation through a linear optical system can be applied to Wigner Distributions in terms of a simple coordinate transformation. This transformation is described by a 4x4 matrix, (almost) identical to the K-matrix.

Definition of Wigner Distributions

Wigner Distributions were originally developed for temporal and spatial coordinates, separately. The time-only Wigner distribution is defined as:

$$W^T(\omega, t) \equiv \int_{-\infty}^{\infty} E\left(t + \frac{t'}{2}\right) E^*\left(t - \frac{t'}{2}\right) \exp(-i\omega t') dt' \quad (28)$$

And the space-only Wigner distribution is defined as:

$$W^S(k, x) \equiv \int_{-\infty}^{\infty} E\left(x + \frac{x'}{2}\right) E^*\left(x - \frac{x'}{2}\right) \exp(-ikx') dx' \quad (29)$$

The Wigner Distributions are real but they can be negative. Here are some nice properties of them: The marginals of the temporal Wigner Distributions yield the pulse intensity vs. time and the spectrum vs. frequency:

$$I(t) = \int_{-\infty}^{\infty} W^T(\omega, t) d\omega \quad (30)$$

$$S(\omega) = \int_{-\infty}^{\infty} W^T(\omega, t) dt$$

The inverse Fourier transforms of the temporal Wigner Distributions yield the pulse field (except for the zeroth-order phase):

$$\begin{aligned} F^{-1}\{W^T(\omega, t)\} &= \frac{1}{2\pi} \int_{-\infty}^{\infty} \int_{-\infty}^{\infty} E\left(t + \frac{t'}{2}\right) E^*\left(t - \frac{t'}{2}\right) \exp(-i\omega t') \exp(i\omega t) d\omega dt' \\ &= E(t) E^*(0) \end{aligned} \quad (31)$$

Wigner Distributions also yield intuitive pictures of the pulse behavior. Figure 2 shows some examples of Wigner Distributions. These properties can be applied to the spatial Wigner distributions.

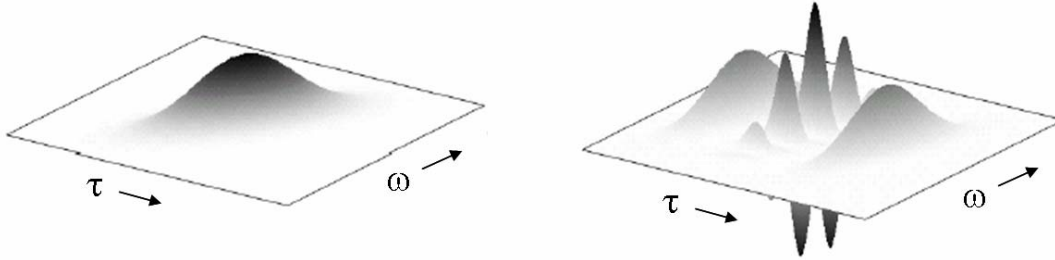


Fig. 2 Wigner Distributions of a linearly chirped Gaussian pulse (left) and a double pulse (right).

In terms of examining spatio-temporal behavior of a beam-pulse, rather than time-only or space-only functions, we would be interested in a formalism, which describes the spatial and temporal pulse behavior at the same time. This is achieved by the “space-time Wigner Distributions”. They are defined as:

$$\begin{aligned} W^{ST}(x, k, t, \omega) &\equiv \int_{-\infty}^{\infty} \int_{-\infty}^{\infty} E\left(x + \frac{x'}{2}, t + \frac{t'}{2}\right) E^*\left(x - \frac{x'}{2}, t - \frac{t'}{2}\right) \\ &\quad \exp(-ikx' - i\omega t') dx' dt' \end{aligned} \quad (32)$$

Note that this definition is useful when the pulse field is expressed in (x,t) domain. However, expressions for other domains follow directly. For example, if the pulse field is expressed in (k,t) domain, we can write:

$$\begin{aligned} W^{ST}(x, k, t, \omega) &\equiv \int_{-\infty}^{\infty} \int_{-\infty}^{\infty} E\left(k + \frac{k'}{2}, t + \frac{t'}{2}\right) E^*\left(k - \frac{k'}{2}, t - \frac{t'}{2}\right) \\ &\quad \exp(-ik'x - i\omega t') dk' dt' \end{aligned} \quad (33)$$

Various integrals of the space-time Wigner Distributions have useful meanings, as for the space-only and time-only ones. For example, the integral of W^{ST} over the wave-vector k gives the temporal Wigner distribution, W^T , for each position, x :

$$\begin{aligned} \int_{-\infty}^{\infty} W^{ST}(x, k, t, \omega) dk &= \int_{-\infty}^{\infty} E(x, t + \frac{t'}{2}) E^*(x, t - \frac{t'}{2}) \exp(i\omega t') dt' \\ &= W^T(x, t, \omega) \end{aligned} \quad (34)$$

Similarly, the integral of W^{ST} over x gives the W^S evaluated at instant t . Integrals over the t and ω follow directly.

Integrals of W^{ST} over two of its variables yield various useful intensity functions:

$$\begin{aligned} \frac{1}{2\pi} \int_{-\infty}^{\infty} \int_{-\infty}^{\infty} W^{ST}(x, k, t, \omega) dk d\omega &= |E(x, t)|^2 \\ \int_{-\infty}^{\infty} \int_{-\infty}^{\infty} W^{ST}(x, k, t, \omega) dk dt &= |E(x, \omega)|^2 \\ \frac{1}{(2\pi)^2} \int_{-\infty}^{\infty} \int_{-\infty}^{\infty} W^{ST}(x, k, t, \omega) dx d\omega &= |E(k, t)|^2 \\ \frac{1}{2\pi} \int_{-\infty}^{\infty} \int_{-\infty}^{\infty} W^{ST}(x, k, t, \omega) dx dt &= |E(k, \omega)|^2 \end{aligned} \quad (35)$$

These intensities are one of the key results of this section, in terms of examining the spatio-temporal couplings. They can be used directly in expressions like Eq. (24) and (16), in order to find normalized coupling values and widths.

The integrals over t - ω and k - x are, however, somewhat less intuitive:

$$\begin{aligned} \frac{1}{2\pi} \int_{-\infty}^{\infty} \int_{-\infty}^{\infty} W^{ST}(x, k, \omega, t) d\omega dt &= \frac{1}{2\pi} \int_{-\infty}^{\infty} W^S(x, k, \omega) d\omega = \overline{W}^S(x, k) \\ \frac{1}{2\pi} \int_{-\infty}^{\infty} \int_{-\infty}^{\infty} W^{ST}(x, k, \omega, t) dx dk &= \frac{1}{2\pi} \int_{-\infty}^{\infty} W^S(x, t, \omega) dx = \overline{W}^T(t, \omega) \end{aligned} \quad (36)$$

where \overline{W}^S and \overline{W}^T are the average Wigner distributions.

Application of the matrix formalism to Wigner Distributions

As mentioned in the beginning of this section, one of the most appealing aspects of Wigner Distributions is that that can conveniently be propagated through a linear optical system, using a matrix formalism, almost identical to the 4x4 K-Matrices. The effect of a linear optical system on the space-time Wigner distributions is simply a coordinate transform and multiplication by a scaling factor. This can be written as:

$$W_{out}^{ST}(x_{out}, k_{out}, t_{out}, \omega_{out}) = m W_{in}^{ST}(x_{in}, k_{in}, t_{in}, \omega_{in}) \quad (37)$$

Where m is the scaling. The coordinate transformation is found using a matrix multiplication:

$$\begin{bmatrix} x_{out} \\ k_{out} \\ t_{out} \\ \omega_{out} \end{bmatrix} = \begin{bmatrix} m_{xx} & m_{xk} & m_{xt} & m_{x\omega} \\ m_{kx} & m_{kk} & m_{kt} & m_{k\omega} \\ m_{tx} & m_{tk} & m_{tt} & m_{t\omega} \\ m_{\omega x} & m_{\omega k} & m_{\omega t} & m_{\omega\omega} \end{bmatrix} \begin{bmatrix} x_{in} \\ k_{in} \\ t_{in} \\ \omega_{in} \end{bmatrix} \quad (38)$$

This transformation matrix is almost identical to the K-matrix, with the replacement of Hertzian frequency with angular frequency and replacement of the angle with k -vector (by multiplication with k_0) for

the components involving these two parameters. Figure 3 shows some example matrices used for transforming the Wigner distributions for various optical systems.

	Lens	Phase Modulator	Dispersive Medium	Grating
Matrix	$\begin{bmatrix} 1 & 0 & 0 & 0 \\ k_0/f & 1 & 0 & 0 \\ 0 & 0 & 1 & 0 \\ 0 & 0 & 0 & 1 \end{bmatrix}$	$\begin{bmatrix} 1 & 0 & 0 & 0 \\ 0 & 1 & 0 & 0 \\ 0 & 0 & 1 & 0 \\ 0 & 0 & \Phi_m \omega_m^2 & 1 \end{bmatrix}$	$\begin{bmatrix} 1 & -z/k_0 & 0 & 0 \\ 0 & 1 & 0 & 0 \\ 0 & 0 & 1 & -k_0''z \\ 0 & 0 & 0 & 1 \end{bmatrix}$	$\begin{bmatrix} \alpha & 0 & 0 & 0 \\ 0 & 1/\alpha & 0 & -\beta/\alpha \\ -\beta & 0 & 1 & 0 \\ 0 & 0 & 0 & 1 \end{bmatrix}$
Scaling factor	1	1	1	1/ α
Parameters	k_0 , Longitudinal wave vector f , Focal length	Φ_m , Amplitude ω_m , Frequency of modulation	z , propagation distance $k_0'' = \partial^2 k / \partial \omega^2$	$\alpha = \frac{\cos \theta_i}{\cos \theta_d}$ $\beta = \frac{2\pi p}{d \cos \theta_d \omega_0}$

Fig. 3 Coordinate transformation matrices for Wigner Distributions for various optical systems.

As a result, the space-time Wigner Distributions can be very useful and time-consuming for analyzing the spatio-temporal pulse behavior, especially for beam-pulses with non-Gaussian shapes. We can examine the spatio-temporal effects of a linear optical system on the pulse following these steps: 1) Find the input Wigner Distribution. 2) Find the corresponding 4x4 coordinate transformation matrix for the system. 3) Find the output Wigner Distribution using Eq. (37). 4) Find the output intensity distributions from Eq. (35). And finally, 5) Find the spatio-temporal couplings using one of the definitions mentioned in the previous section.

References

1. A. E. Siegman, *Lasers* (University Science Books, Sausalito, CA, 1986).
2. R. L. Fork, O. E. Martinez, and J. P. Gordon, "Negative dispersion using pairs of prisms," *Opt. Lett.* **9**, 150-152 (1984).
3. Z. Bor, B. Racz, G. Szabo, M. Hilbert, and H. A. Hazim, "Femtosecond Pulse Front Tilt Caused by Angular-Dispersion," *Opt Eng* **32**, 2501-2504 (1993).
4. J. Hebling, "Derivation of the pulse front tilt caused by angular dispersion," *Optics and Quantum Electronics* **28**, 1759-1763 (1996).
5. S. Akturk, X. Gu, E. Zeek, and R. Trebino, "Pulse-front tilt caused by spatial and temporal chirp," *Opt. Express* **12**, 4399-4410 (2004).
6. A. G. Kostenbauder, "Ray-Pulse Matrices: A Rational Treatment for Dispersive Optical Systems," *IEEE J. Quantum Electron.* **26**, 1148-1157 (1990).
7. S. Akturk, X. Gu, P. Gabolde, and R. Trebino, "The general theory of first-order spatio-temporal distortions of Gaussian pulses and beams," *Opt. Express* **13**, 8642-8661 (2005).